Corrections to absorbed dose calculations for tissue inhomogeneities

Marc R. Sontag and J. R. Cunningham

Ontario Cancer Institute, Toronto, Ontario M4X 1K9, Canada

(Received 25 October 1976; accepted for publication 4 March 1977)

Traditional methods for correcting for the presence of tissue inhomogeneities may produce errors as great as 10% at points within or close to the inhomogeneity. A more accurate method is presented which employs tissue–air ratios raised to some power dependent on the relative electron densities of the inhomogeneities involved. Corrections may be made for points that lie within or below an inhomogeneity as well as for multiple inhomogeneities. Measurements were made in phantoms containing aluminum or cork inhomogeneities. Agreement between measured and predicted results was usually within 2%–3%.

I. INTRODUCTION

In recent years, there has been a proliferation of CT scanners as a valuable diagnostic tool in radiology. More recently, attention has been turned to the possible application of these devices to radiotherapy treatment planning. It is now possible to process the CT image so as to obtain an accurate cross-sectional map of the patient's shape, as well as the location and density of internal organs.

In regions where dose calculations would be affected by tissue inhomogeneities, accuracy has been limited by inability to define correctly both the geometry and density of these structures. The availability of CT scanners and similar devices has altered the situation so that now the limiting factor is in fact the algorithm used to allow for the presence of the tissue inhomogeneities when making dose calculations.

The degree of accuracy needed for clinical acceptability is not known and has been the subject of considerable debate. Evidence has been presented[1,2] that an increase of 10% above the "optimal" dose has produced an observable increase of tissue necrosis, while a reduction in the dose of 10% greatly decreases the chance of local control. It has been suggested by these authors that a reasonable degree of accuracy for clinical acceptability should therefore be ±5% of the "optimal" due to all sources of error and ±2% due to each component. If we conservatively accept these recommendations, then ±2% is the desired goal in the calculative portion. It will be shown that traditional methods used to correct for tissue inhomogeneities in many cases fail to meet this requirement, even with the availability of accurate information provided by CT scanners. An algorithm based on work by Batho[3] will be presented which the authors believe will, in most cases, meet this desired goal. Further, the method is simple enough to allow corrections for tissue inhomogeneities to be made by either hand or computer calculations in times comparable to traditional, less accurate methods.

II. EFFECT OF AN INHOMOGENEITY ON THE DOSE TO A POINT

The calculation of a dose to a point such as P in Fig. 1(a) involves the determination of the quantity of energy deposited within the region of that point. This will be proportional to the photon energy fluence there. This fluence has a primary component, which consists of photons that have not undergone any interaction in the phantom en route to point P, and a scattered or secondary component, which consists of photons reaching point P as a result of one or more interactions occurring away from the immediate region of point P. Figure 1(a) illustrates these phenomena, in which a primary photon and two singly scattered photons reach point P in a homogeneous medium of density $\rho = 1.00$ g/cm^3. The introduction of an inhomogeneity may have an effect on one or both components as suggested in Fig. 1(b). In this case, the primary photons reaching point Q will be attenuated differently (from those reaching point P) because of the introduction of non-unit-density material in their path. The scattered radiation will also be affected. In fact, the effects on the primary and scattered components are somewhat counterbalancing. A low density ($\rho < 1.00$ g/cm^3) inhomogeneity, for example, will cause a decrease in attenuation of the primary component resulting in an increase in the dose at a given point. At the same time, the mass of the scattering material will decrease, causing a decrease in the dose. This counterbalancing will be most evident with a geometry similar to that shown in Fig. 1(c) where the point of consideration is within the non-unit-density material. For most points, the effect of the inhomogeneity will be larger on the primary than on the scattered component, and the net effect will be an increase in the dose at a point influenced by a low-density inhomogeneity. High-density inhomogeneities ($\rho > 1.00$ g/cm^3) will produce the opposite effect. As with low-density inhomogeneities, the effect on the primary usually predominates, so for points influenced by high-density inhomogeneities there will, in general, be a net decrease in the dose.

The usual procedure in allowing for the effects of inhomogeneities in dose calculations is to assume first that the irradiated medium is homogeneous and water or muscle tissue equivalent in composition and then obtain a correction factor CF to account for the presence of the inhomogeneity. For example, the dose at point Q in Fig. 1(b) may be obtained from the dose at point P thus:

$$D_Q = D_P \times \mathrm{CF}. \quad (1)$$

There are three methods in common use for calculating

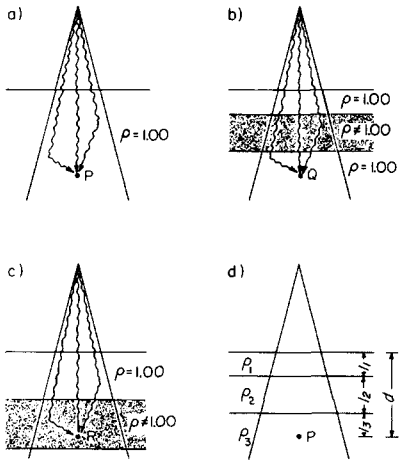

FIG. 1. The dose to point P in a homogeneous tissue-equivalent medium (a) is a result of both primary and scattered radiation. Introduction of an inhomogeneity (b) and (c) alters the attenuation of the primary as well as the magnitude of scatter; the former a function of thickness of the inhomogeneity, while the latter is also a function of the position and lateral dimensions of the inhomogeneity. Traditional methods (d) consider only effects on the primary by calculating an effective thickness.

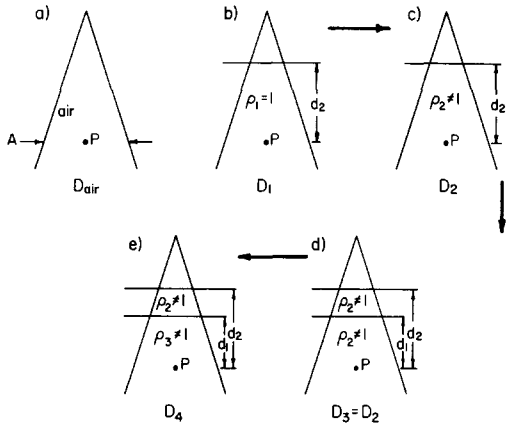

FIG. 2. Tissue-air ratios may be used as modifying factors to alter the dose when point P in air (a) is sequentially replaced with different slabs of medium until point P lies at a depth of d_1 within a medium of density ρ_3 below another medium of thickness $d_2 - d_1$ of density ρ_2.

the appropriate correction factor. They have been called the "effective attenuation coefficient method," the "isodose shift method," and the "effective SSD" method. These and similar methods are discussed in the literature[4-10] and are summarized in a recent ICRU report.[11] All involve the calculation of an effective or radiological thickness.

$$d_{\text{eff}} = l_1\rho_1 + l_2\rho_2 + l_3\rho_3 + \cdots, \tag{2}$$

where l_1 is the thickness of the region with density ρ_1, etc., as shown in Fig. 1(d). The difference between d_{eff} and the actual depth d is used to calculate an effective increased (or decreased) attenuation and takes no account of the distance the inhomogeneity is in front of the point of calculation. No account is therefore taken of the alteration caused in the geometry of the scattering conditions. This neglect may cause errors of as much as 10% for certain geometries, an error that is much greater than the 2% being sought. This problem will be examined in greater detail with experimental evidence later in this paper. If the point of calculation is sufficiently far from the inhomogeneity so that scatter arising from the inhomogeneity does not reach the point, then the scattering mass does not change and hence is no longer a factor. In this situation, the linear attenuation, isodose shift, and effective SSD methods will predict the dose with clinically acceptable accuracy. As will be seen later, however, in many cases a significant proportion of the points do receive scatter arising from the inhomogeneity so a more satisfactory correction algorithm must be found.

III. DERIVATION OF A POWER-LAW TISSUE-AIR-RATIO CORRECTION FACTOR

Batho[3] and later Young and Gaylord[5,12] have proposed a method for correcting for the presence of tissue inhomogeneities employing tissue-air ratios and electron densities of the inhomogeneities. This method indirectly accounts for part of the change in the scattering geometry neglected by the correction methods discussed in the previous section. The original form of this correction method[3,5,12] allows only for the case where the point of calculation is below an inhomogeneity, but within tissue-like material ($\rho = 1$). It was shown experimentally by Young and Gaylord to be very successful in predicting the alteration in dose for this case. In Sec. IV, a more general form of this correction factor will be derived that will allow for correction of the dose to points within an inhomogeneity as well as below it. In addition, geometries that include multiple inhomogeneities will also be examined.

Let point P of Fig. 2(a) be a point in air irradiated as shown. Let the absorbed dose in a small mass of tissue at this point be D_{air}. In Fig. 2(b), point P is at the same location with respect to the beam but is within a homogeneous tissue-like phantom. It is at a depth d_2 below the surface and the field dimensions at this point are denoted by A. The dose D_1 at point P is given by the definition of tissue-air ratio as

$$D_1 = D_{\text{air}} \cdot T(d_2,A). \tag{3}$$

The tissue-air ratio is the modifying factor describing how the dose to a small mass of tissue at such a point in air is altered by now being located within a tissue-like medium. If we next imagine the density of the medium to be doubled [Fig. 2(c)], then in the same volume there will be double the number of atoms, double the number of electrons, and hence double the number of all interactions. Doubling these means that the modifying factor should be applied twice in a multiplicative fashion.[13] The new dose at point P would then be

$$\begin{aligned} D_2 &= D_{\text{air}} \cdot [T(d_2,A) \cdot T(d_2,A)] \\ &= D_{\text{air}} \cdot [T(d_2,A)]^2. \end{aligned} \tag{4}$$

Tripling the number of interactions by tripling the density would result in the modifying factor being cubed, and so forth.

From Eq. (4), it follows that if ρ volumes of media of density 1.00 are "compacted" into a single volume of physical density ρ, the dose at point P will be

$$D_2 = D_{\text{air}} \cdot [T(d_2,A)]^{\rho}. \tag{5}$$

In the case of ^{60}Co and x-ray beams of comparable energy, where Compton interactions predominate, the relative electron density (compared to that of tissue) should be used instead of the physical density.

$$D_2 = D_{air} \cdot [T(d_2,A)]^{\rho_e}. \quad (6)$$

At lower energies, where photoelectric interactions predominate or, at higher energies where pair production is important, there is also an atomic number dependence. At these energies, it is no longer sufficient to use ρ_e. In what follows, for simplicity, we will use ρ to signify ρ_e, the relative electron density. From Eqs. (3) and (5) we may derive a relation between the dose in the tissue-equivalent medium and that in the medium with relative electron density ρ_2.

$$D_2/D_1 = T(d_2,A)^{\rho_2}/T(d_2,A). \quad (7)$$

We wish to derive a more general expression for the dose D_4 of Fig. 2(e) where the point P is in a region of density ρ_3 and below a region of density ρ_2, neither of the regions being tissue-like. Consider first the two layers shown in Fig. 2(d). Both have density ρ_2. The dose D_3 must be equal to D_2 since the two conditions are identical. We could rewrite Eq. (7) as a product of two terms:

$$\frac{D_3}{D_1} = \frac{T(d_1,A)^{\rho_2}}{T(d_2,A)} \cdot \frac{T(d_2,A)^{\rho_2}}{T(d_1,A)^{\rho_2}}. \quad (8)$$

The first term corrects for the change in density of the lower portion, replacing tissue-like material of thickness d_2 with material of density ρ_2 and thickness d_1, and the second corrects for the addition of a layer of thickness $(d_2 - d_1)$, density ρ_2.

If next the bottom portion (thickness d_1) is changed to a new material of density ρ_3,

$$D_4/D_3 = T(d_1,A)^{\rho_3}/T(d_1,A)^{\rho_2} \quad (9)$$

and the overall correction factor is

$$\frac{D_4}{D_1} = \frac{T(d_1,A)^{\rho_3-\rho_2}}{T(d_2,A)^{1-\rho_2}}. \quad (10)$$

The general form of the equation for the correction factor in which the inhomogeneities have the same effective atomic number as muscle tissue is

$$CF = \frac{T(d_1,A)^{\rho_a-\rho_b}}{T(d_2,A)^{1-\rho_b}}, \quad (10a)$$

where ρ_a is the density of the material in which point P lies at a depth d_1 below its surface and ρ_b is the density of an overlying material of thickness $(d_2 - d_1)$.

In the case in which point P is in tissue-like material ($\rho_a = 1$) and below non-tissue-like material, the equation reduces to

$$CF = [T(d_1,A)/T(d_2,A)]^{1-\rho_b}, \quad (10b)$$

which is the equation given by Batho.[3] If the point lies within a non-tissue-like region of density ρ_a, overlain by tissue-like material ($\rho_b = 1$), the correction factor reduces to

$$CF = T(d_1,A)^{\rho_a-1}. \quad (10c)$$

The above development does not, however, account for the differences in atomic number between the non-tissue-like material and tissue. In cases where the effective atomic number of the inhomogeneity is different than muscle tissue, the correction factor CF must be further modified by a ratio of mass energy absorption coefficients. In a more general form, the correction factor for the dose at a point within a region of density ρ_a, overlain by a region of density ρ_b is

$$CF = \frac{T(d_1,A)^{\rho_a-\rho_b}}{T(d_2,A)^{1-\rho_b}} \cdot \frac{(\mu_{en}/\rho)_{\rho_a}}{(\mu_{en}/\rho)_{\rho_b}}. \quad (11)$$

We will call this expression the "generalized Batho" equation. In deriving it, a number of assumptions have been made:

(1) Only geometry above the point is examined. It is assumed that the material below the point is the same as that in which the point lies. The maximum error that could result from this would occur if the point of calculation were just at the exit surface of a phantom in which case there would be a loss of backscattering material and the dose would be reduced by a factor somewhat less than the reciprocal of the peak scatter factor. In the more general case, an additional correction would be required to account for the difference in backscatter between the material in which the point lies and that for tissue. In most cases, the error is considered negligible.

(2) The effect of an inhomogeneity on the dose to a point is independent of the thickness of tissue ($\rho = 1$) above the inhomogeneity.

(3) Electronic equilibrium exists. At locations near an interface this will be disturbed and could cause appreciable errors, particularly for very-high-energy radiation, where the secondary electrons may travel several centimeters.

(4) The lateral dimensions of all regions are assumed to be at least those of the beam.

The magnitude of these errors will have to be examined in the future. This paper deals only with the basic equation.

TABLE I. Physical properties of attenuating media: ρ is the measured physical density of the material. μ is the linear attenuation coefficient of the material for ^{60}Co energy and was determined by narrow beam attenuation measurements. ρ_e is the ratio of the electron density of the material to the electron density of water. At ^{60}Co energy, $\rho_e = \mu_{MAT}/\mu_{H_2O}$ Lucite was not used in the experiments and is included for information purposes only.

Medium	ρ (g cm^{-3})	ρ_e	μ (cm^{-1})
Polystyrene	1.04	1.02	0.065
Aluminum	2.70	2.34	0.149
Cork	0.24	0.25	0.016
Lucite	1.18	1.15	0.0735

IV. EXPERIMENTAL METHODS AND RESULTS

Measurements were made primarily on an AECL Theratron CTS-780 ^{60}Co unit. Table I summarizes the phantom media used. Polystyrene was used as the tissue-equivalent medium because of its ease of use with the other media as well as its physical similarity to muscle tissue. Cork was chosen to approximate lung. Although this particular cork has a density lower than that of lung, its porous nature and atomic number are similar to lung. Aluminum was chosen to approximate bone. It has the same atomic number and its rel-

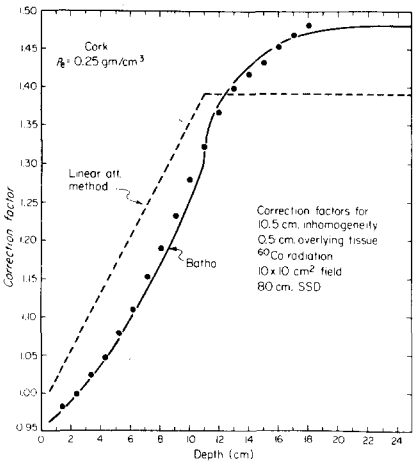

FIG. 3. Correction factors for points along the beam axis lying both within and below a 10.5-cm cork inhomogeneity.

atively high density provides a good test of the equation. Lucite can be used either as a tissue-equivalent medium, if the appropriate corrections are made, or as a high-density inhomogeneity that is only moderately different from the density of muscle tissue. All the attenuators used were flat and had lateral dimensions larger than the largest beam size (15 × 15 cm^2) with the exception of those used for the experiment described in Fig. 7(b). Measurements were recorded with either Harshaw TLD-100 lithium-fluoride powder encapsulated in a gelatin capsule or a Farmer ionization chamber connected to a Keithley electrometer and digital voltmeter. Relative readings were used, in which a reading was taken with and without the presence of an inhomogeneity, all other conditions being the same; no absolute calibration of either dosimeter was necessary. All readings with the Farmer chamber were taken without the buildup cap. No corrections using mass energy absorption coefficient as in Eq. (11) were made either to the instrument readings or the calculations.

A. Measurements using cork

Figure 3 shows results obtained with a phantom consisting of a 0.5-cm slab of polystyrene followed by 10.5 cm of cork followed by several centimeters of polystyrene. The diagram shows a graph of correction factors versus depth below the surface of the composite phantom. The correction factors derived from measurements were obtained by taking readings in the phantom just described and dividing them by readings obtained in a homogeneous polystyrene phantom. The dashed line was obtained using a simple correction of 5%/cm of "missing" tissue, i.e., 3.75%/cm of "lung tissue" having relative density 0.25, while the solid line was obtained from the "generalized Batho" equation, CF = $(d_1,A)^{-0.75}$, where the depth d_1 is the depth of point P in cork [Eq. (10c)]. At ^{60}Co energy, it is necessary to extrapolate the tissue-air-ratio values to depths less than 0.5 cm so that $T(d_{<0.5},A) > T(d_{0.5},A)$.

Both the measurements and the "Batho" equation showed that, in the first few centimeters of the cork, the correction factor fell below 1.00, indicating that the "dose" in cork can be lower than the "dose" for the same depth in polystyrene. Similar effects have been noted for orthovoltage x rays.[14] This effect is assumed to be due to the marked decrease in the scattered radiation. It is not fully compensated by a decrease in the attenuation of the primary photons. For points deeper in cork, although there is less scattered radiation, the attenuation of the primary continues to decrease and the net result is an increase above 1.0 in the correction factor and a continuing increase in the correction factor with increasing depth within the inhomogeneity. At a depth in cork of 2–3 cm these two effects are equal in magnitude and the correction factor versus depth is fairly constant until near the cork–polystyrene interface at the bottom of the inhomogeneity. Here the experimental points increase somewhat more rapidly due likely to increased backscatter from the polystyrene. Again, within unit-density material, the correction factor continues to increase for a few centimeters more and then tends to level off. This is because progressively more of the scattered photons reaching the calculation point arise from the polystyrene rather than the cork. For points well beyond the inhomogeneity, the correction factor is primarily dependent on changes in the primary component of the radiation; for these points, correction factors predicted by the linear attenuation method are in good agreement with experimental values.

It can be seen that the dose behavior for points within or near an inhomogeneity is much more complicated than could be described by a linear attenuation method and that, for a case such as this, errors well in excess of 10% could result. The Batho-type correction, on the other hand, gives exceedingly good agreement with experimental results.

Figure 4 indicates variation of the correction factor as a function of depth for points within a homogeneous cork phantom. For a given depth, the correction factor increases in magnitude as the field size decreases. Trends evident in Fig. 3 are also apparent here. The correction factor falls below 1.00 in the first 2–3 cm and then continues to rise. The measured values were usually within 1% of the values predicted by the generalized Batho equation, although the measured values were always higher. It is not clear whether this trend is an experimental artifact, an incorrect estimation of ρ_e, or a small inadequacy of the Batho model. A third phantom containing a 5.7-cm cork inhomogeneity was con-

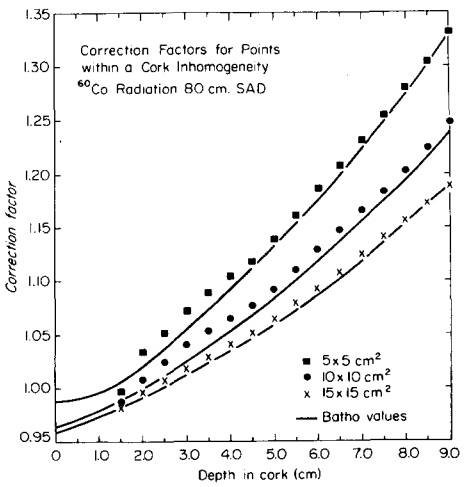

FIG. 4. Variation of the correction factor as a function of depth for points along the beam axis within a cork phantom.

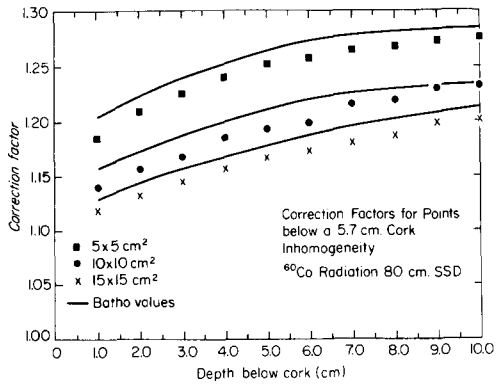

FIG. 5. Variation of the correction factor as a function of depth for points along the beam axis beneath a 5.7-cm cork inhomogeneity.

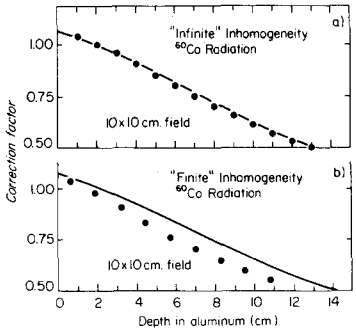

FIG. 7. Comparison of the correction factor for points within a phantom composed entirely of aluminum (30-cm width × 30-cm length × 30-cm depth) (a) and slabs of aluminum with one lateral dimension reduced (3-cm width × 30-cm length × 30-cm depth) (b) laterally enclosed by tissue-equivalent material. All readings were made in aluminum along the beam axis, which was centered in the middle of aluminum. The beam size in (a) was always 10 × 10 cm^2 at the depth of measurement. In (b), the field size was defined at the phantom surface (0-cm depth), producing field sizes slightly larger than 10 × 10 cm^2 at greater depths. This explains the slightly different shape of the two solid lines, which are the correction factors predicted by the Batho method.

structed (Fig. 5) and correction factors were determined for points beneath the cork. Agreement between the Batho and measured values is again good although, in this geometry, the measured values were always low. It appears that for points within and beneath a cork inhomogeneity, agreement between measured and Batho values does not vary greatly as a function of field size.

B. Measurements using aluminum

The use of a high-density inhomogeneity should produce trends opposite to those for the low-density inhomogeneity. Figure 6 illustrates this situation; a 3.7-cm aluminum inhomogeneity lies beneath 1.0 cm of overlying unit-density material. There is an initial rise of the correction factor above 1.00 because of the sudden increase in density of the scattering material.

With increasing depth, the effect on the primary component becomes predominant and the correction factor drops below 1.00. Agreement between measured values and the values predicted by the generalized Batho equation are not quite as good as was the case with cork. This is to be expected since there is a greater difference in density between aluminum and polystyrene than cork and polystyrene. However, agreement was usually within ±2%, although in some cases as bad as 4%–5% for points within the aluminum for large field sizes (15 × 15 cm^2). Due to aluminum's relatively high density, it is likely that not all the scatter arising from the aluminum may reach a particular point for which a correction factor is calculated. This effect becomes more evident with increasing field size. For points beneath the aluminum, where scatter considerations are no longer as important, agreement was usually within ±1%. It must be noted that bone, which the aluminum is meant to approximate, is not as dense, so that this effect will not be as severe. As was the case with cork, there appears to be little or no field-size effect on the agreement between the measured correction factor and Batho-predicted correction factor for points beneath the aluminum inhomogeneity.

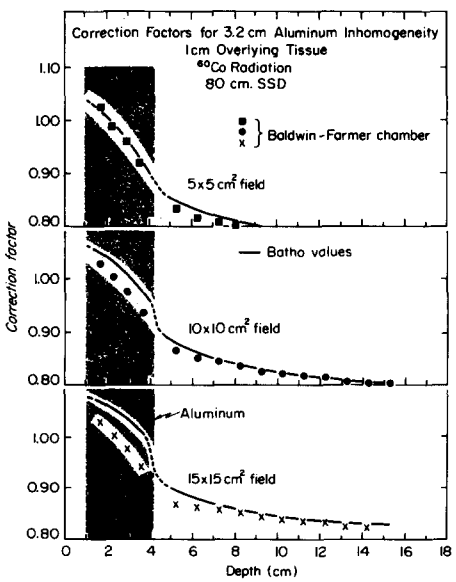

FIG. 6. Variation of the correction factor as a function of depth for points along the beam axis both within and below a 3.2-cm aluminum inhomogeneity.

A basic assumption in the Batho-type model is that the inhomogeneities have lateral dimensions larger than the beam size. However, in clinical situations the lateral dimensions might be smaller than the beam. In Fig. 7, measurements were made using a 10 × 10-cm^2 ^{60}Co beam. For the top graph, measurements were made using an "infinite" inhomogeneity of aluminum (lateral dimensions of 30 × 30 cm^2 and "infinite" thickness). As before, agreement between measured values and predicted values was ±2%. In the lower graph, a "finite" aluminum inhomogeneity (lateral dimensions of 3 × 30 cm^2 and infinite thickness), laterally surrounded by polystyrene was used. The decrease in the size of one of the lateral dimensions of aluminum and replacement of it with the less dense polystyrene has the effect of markedly decreasing the number of scattering sites, and hence the scatter reaching a point in the center of the aluminum. Since the thickness of the aluminum was not altered, there is no change in the differential attenuation of the primary photons.

The next effect will be a decrease in the dose to a point within the inhomogeneity and, hence, a decrease in its correction factor. The Batho model will not sense such a change in the lateral dimensions of the inhomogeneity, since it looks at the beam size only. This will cause an overestimation of the dose by as much as 8%–10%. To avoid this problem, a consideration of the lateral dimensions of both the beam and inhomogeneity is necessary, which is not possible using the generalized Batho equation in its present form.

Another problem is encountered in the use of therapy energies higher than ^{60}Co. Compton interactions become less predominant as the photon energy increases, causing a decrease in the relative percentage of scatter. This probably will affect the accuracy of the dose predicted by the generalized Batho equation, which assumes 100% Compton interactions. This might be circumvented by a separate analysis of the primary and scattered components.

C. Multiple inhomogeneities

Measurements were made using multiple inhomogeneities. This usually involved two adjacent slabs of aluminum and Lucite. The trends and magnitude of error seen with single inhomogeneities were also seen with multiple inhomogeneities, indicating that the generalized Batho equation for single inhomogeneities is a correct extension of the original Batho equation. In the case of determining the correction factor to a point affected by two or more nonadjacent inhomogeneities, the correct procedure is to determine a correction factor for each individual inhomogeneity (as though the others were not there) and then to calculate a composite correction factor which is the product of the individual correction factors.

V. DISCUSSION AND CONCLUSIONS

The generalized Batho method predicts the dose to most points affected by one or more inhomogeneities with suitable accuracy to be clinically acceptable. It is far more accurate for predicting the dose to points that lie within an inhomogeneity than the more traditional linear attenuation, isodose shift and effective SSD methods. The basic shortcoming of the Batho method is the fact that it only indirectly accounts for scatter effects, producing some error for inhomogeneities of small lateral dimensions and for high-energy x rays. It is felt by the authors, however, that this method is currently the best practical method available to correct for the presence of tissue inhomogeneities. The generalized Batho method is currently the algorithm used in program DENCOR, which is part of the TP-11 treatment-planning system, marketed by Atomic Energy of Canada Limited. It is hoped that a future version of the program will incorporate an algorithm that will correct for the problems encountered in the analysis of the scatter component previously discussed.

ACKNOWLEDGMENTS

The financial assistance of the National Cancer Institute and the Medical Research Council of Canada is gratefully acknowledged.

[1]L. J. Shukovsky, Am. J. Roentgenol. **108,** 27 (1970).
[2]D. F. Herring and D. M. J. Compton, Br. J. Radiol. Sp. Rep. No. 5, 51 (1970).
[3]H. F. Batho, J. Can. Assoc. Radiol. **15,** 79 (1964).
[4]ICRU Rep. No. 10d (1962).
[5] M. E. J. Young, *Radiological Physics* (Academic, New York, 1967), 2nd ed., pp. 412–425.
[6]J. van de Geijn, Comput. Programs Biomed. **2,** 153 (1972).
[7]J. van de Geijn, Comput. Programs Biomed. **2,** 169 (1972).
[8]J. Weinkam and T. Sterling, Comput. Programs Biomed. **2,** 178 (1972).
[9]J. Milan and R. E. Bentley, Br. J. Radiol. **47,** 115 (1974).
[10]J. M. Wilkinson and W. J. Redmond, Br. J. Radiol. **48,** 732 (1975).
[11]ICRU Rep. No. 24 (1976).
[12]M. E. J. Young and J. D. Gaylord, Br. J. Radiol. **43,** 349 (1970).
[13]Although this is not rigorously true; it is a good approximation.
[14]M. Cohen, Br. J. Radiol. **28,** 669 (1955).